Synthesis and Photophysical Properties of Mono(2,2′,2″-terpyridine) Complexes of Ruthenium(II)

Benjamin J. Coe, David W. Thompson, Christopher T. Culbertson, Jon R. Schoonover, and Thomas J. Meyer*

Department of Chemistry, University of North Carolina at Chapel Hill, Chapel Hill, North Carolina 27599-3290

Received March 16, 1994[⊗]

A series of $[Ru(tpy)(X)(Y)(Z)]^{n+}$ complexes have been synthesized (tpy = 2,2′,2″-terpyridine: X = triphenylphosphine (PPh_3); *trans* Y = Z = trifluoroacetate ($CF_3CO_2^-$), $n = 0$ (**1**); *trans* Y = Z = 4-ethylpyridine (4-Etpy), $n = 2$ (**2**); *trans* Y = Z = 4-(dimethylamino)pyridine (DMAP), $n = 2$ (**3**); Y = 4-Etpy, Z = chloride (Cl^-), $n = 1$ (**4**); *cis* Y = Z = 4-Etpy, $n = 2$ (**5**); X = Cl^-; *trans* Y = Z = 4-Etpy, $n = 1$ (**6**); X = Y = Z = 4-Etpy, $n = 2$ (**7**)) and isolated as their PF_6^- salts. UV−visible spectroscopic and electrochemical studies have been conducted and photochemical and photophysical properties of representative examples determined. Emission, absorption, and electrochemical properties depend on the nonchromophoric ligands and the coordination geometry. The complexes investigated emit in 4:1 (v/v) EtOH/MeOH glasses at 77 K and have lifetimes which range from 1.1 to 11.0 μs depending on the ancillary ligands. Through a combination of emission spectral fitting and resonance Raman measurements on $[Ru(tpy)_2](PF_6)_2$, the acceptor characteristics of tpy as a chromophoric ligand have been analyzed. At room temperature the Ru(II) mono-tpy complexes are short-lived, weak emitters. Emission quantum yields and lifetimes for $[Ru(tpy)(4\text{-}Etpy)_3](PF_6)_2$ (**7**) and $[Ru(tpy)_2](PF_6)_2$ in 4:1 (v/v) EtOH/MeOH are strongly temperature dependent from $T = 90-270$ K. These results are consistent with the existence of low-lying dd states which are responsible for the short excited state lifetimes at room temperature and the appearance of ligand-loss photochemistry for **7**.

Introduction

The metal to ligand charge transfer (MLCT) excited states of polypyridine complexes have been used extensively as a chromophoric basis for the study of photoinduced electron and energy transfer in molecular assemblies.[1] Many of these assemblies have resulted from coordination chemistry which allows only a limited degree of control over molecular structure. Further development requires more complete control over structure by using precisely defined synthetic strategies. Recent reports featuring such an approach concern Ru(II) and Os(II) bis(terpyridine) complexes,[2] Ru(II) functionalized amino acid assemblies,[3] and oligometallic arrays containing bridging ligands based on both bipyridines[4] and terpyridines.[5]

There are numerous studies on the photochemistry and photophysics of ruthenium(II) complexes with 2,2′-bipyridine (bpy) as the acceptor ligand[6] but relatively few reports concerning related 2,2′,2″-terpyridine (tpy) complexes.[7-20] This is largely because $[Ru(tpy)_2]^{2+}$ and its derivatives exhibit very short excited state lifetimes at room temperature in solution (for

[⊗] Abstract published in *Advance ACS Abstracts,* February 1, 1995.

(1) (a) Meyer, T. J. *Acc. Chem. Res.* **1989**, *22*, 163. (b) Belser, P. *Chimia* **1990**, *44*, 226. (c) Meyer, T. J. *Pure Appl. Chem.* **1990**, *62*, 1003. (d) Balzani, V.; Scandola, F. *Supramolecular Photochemistry*; Ellis Horwood: Chichester, U.K., 1991.

(2) (a) Collin, J.-P.; Guillerez, S.; Sauvage, J.-P.; Barigelletti, F.; De Cola, L.; Flamigni, L.; Balzani, V. *Inorg. Chem.* **1991**, *30*, 4230. (b) Collin, J.-P.; Guillerez, S.; Sauvage, J.-P.; Barigelletti, F.; De Cola, L.; Flamigni, L.; Balzani, V. *Inorg. Chem.* **1992**, *31*, 4112.

(3) (a) Mecklenburg, S. L.; Peek, B. M.; Erickson, B. W.; Meyer, T. J. *J. Am. Chem. Soc.* **1991**, *113*, 8540. (b) Mecklenburg, S. L.; Peek, B. M.; Schoonover, J. R.; McCafferty, D. G.; Wall, C. G.; Erickson, B. W.; Meyer, T. J. *J. Am. Chem. Soc.* **1993**, *115*, 5479.

(4) (a) Campagna, S.; Denti, G.; Serroni, S.; Ciano, M.; Balzani, V. *J. Am. Chem. Soc.* **1992**, *114*, 2944. (b) Belser, P.; von Zelewsky, A.; Frank, M.; Seel, C.; Vögtle, F.; De Cola, L.; Barigelletti, F.; Balzani, V. *J. Am. Chem. Soc.* **1993**, *115*, 4076. (c) Juris, A.; Balzani, V.; Campagna, S.; Denti, G.; Serroni, S.; Frei, G.; Güdel, H. U. *Inorg. Chem.* **1994**, *33*, 1491 and references therein.

(5) (a) Constable, E. C.; Cargill-Thompson, A. M. W. *J. Chem. Soc., Dalton Trans.* **1992**, 3467. (b) Newkome, G. R.; Cardullo, F.; Constable, E. C.; Moorefield, C. N.; Cargill-Thompson, A. M. W. *J. Chem. Soc., Chem. Commun* **1993**, 925. (c) Grosshenny, V.; Ziessel, R. *J. Organomet. Chem.* **1993**, *453*, C19. (d) Sauvage, J.-P.; Collin, J.-P.; Chambron, J.-C.; Guillerez, S.; Coudret, C.; Balzani, V.; Barigelletti, F.; De Cola, L.; Flamigni, L. *Chem. Rev.* **1994**, *94*, 993. (e) Constable, E. C.; Cargill-Thompson, A. M. W. *J. Chem. Soc., Dalton Trans.* **1994**, 1409.

(6) (a) Bryant, G. M.; Ferguson, J. E.; Powell, H. K. J. *Aust. J. Chem.* **1971**, *24*, 257. (b) Kalyanasundaram, K. *Coord. Chem. Rev.* **1982**, *46*, 159. (c) Watts, R. J. *J. Chem. Educ.* **1983**, *60*, 834. (d) Meyer, T. J. *Pure Appl. Chem.* **1986**, *58*, 1193. (e) Juris, A.; Balzani, V.; Barigelletti, F.; Campagna, S.; Belser, P.; von Zelewsky, A. *Coord. Chem. Rev.* **1988**, *84*, 85. (f) DeArmond, M. K.; Myrick, M. L. *Acc. Chem. Res.* **1989**, *22*, 364. (g) Krausz, E.; Ferguson, J. *Prog. Inorg. Chem.* **1989**, *37*, 293.

(7) (a) Klassen, D. M.; Crosby, G. A. *J. Chem. Phys.* **1968**, *48*, 1853. (b) Demas, J. N.; Crosby, G. A. *J. Am. Chem. Soc.* **1971**, *93*, 2841. (c) Stone, M. L.; Crosby, G. A. *Chem. Phys. Lett.* **1981**, *79*, 169. (d) Agnew, S. F.; Stone, M. L.; Crosby, G. A. *Chem. Phys. Lett.* **1982**, *85*, 57.

(8) Fink, D. W.; Ohnesorge, W. E. *J. Am. Chem. Soc.* **1969**, *91*, 4995.

(9) Lin, C.-T.; Böttcher, W.; Chou, M.; Creutz, C.; Sutin, N. *J. Am. Chem. Soc.* **1976**, *98*, 6536.

(10) (a) Young, R. C.; Meyer, T. J.; Whitten, D. G. *J. Am. Chem. Soc.* **1976**, *98*, 286. (b) Nagle, J. K.; Meyer, T. J. *Inorg. Chem* **1984**, *23*, 3663.

(11) Young, R. C.; Nagle, J. K.; Meyer, T. J.; Whitten, D. G. *J. Am. Chem. Soc.* **1978**, *100*, 4773.

(12) Braterman, P. S. *Chem. Phys. Lett.* **1984**, *104*, 405.

(13) Kirchoff, J. R.; McMillin, D. R.; Marnot, P. A.; Sauvage, J.-P. *J. Am. Chem. Soc.* **1985**, *107*, 1138.

(14) Winkler, J. R.; Netzel, T. L.; Creutz, C.; Sutin, N. *J. Am. Chem. Soc.* **1987**, *109*, 2381.

(15) Berger, R. M.; McMillin, D. R. *Inorg. Chem* **1988**, *27*, 4245.

(16) Suen, H.-F.; Wilson, S. W.; Pomerantz, M.; Walsh, J. L. *Inorg. Chem* **1989**, *28*, 786.

(17) Hecker, C. R.; Gushurst, A. K. I.; McMillin, D. R. *Inorg. Chem.* **1991**, *30*, 538.

(18) Beley, M.; Collin, J.-P.; Sauvage, J.-P.; Sugihara, H.; Heisel, F.; Miehe, A. *J. Chem. Soc., Dalton Trans.* **1991**, 3157.

0020-1669/95/1334-3385$09.00/0

$[Ru(tpy)_2]^{2+*}$ $\tau = 250$ ps in water).[14] The origin of these short lifetimes continues to be debated. Explanations have been advanced on the basis of enhanced nonradiative decay due to solvent interactions,[11] thermally activated, nonradiative decay via metal-centered dd excited states,[8,13,17,21] or efficient decay through low-energy, intramolecular vibrations of the tpy ligand.[19]

This paper contains two interwoven themes. The primary objective was an attempt to establish general synthetic routes to molecular assemblies based on the *trans* geometry at Ru(II) in mono-tpy complexes. By using the complex *trans*-Ru(tpy)-$(PPh_3)Cl_2$ as a precursor, which is readily prepared from Ru-$(tpy)Cl_3$,[22] we sought to find ways to replace the chlorides by pyridyl ligands with the ultimate aim of achieving stepwise substitution while maintaining the *trans* geometry. The second goal was to revisit excited state dynamics based on tpy as the acceptor ligand and to shed new light on the mechanism of efficient nonradiative decay in Ru(II)−tpy complexes.

Experimental Section

Materials, Synthetic Procedures, and Purification. The complexes $Ru(tpy)Cl_3$ and *trans*-$Ru(tpy)(PPh_3)Cl_2$ and the salt $[Ru(tpy)_2](PF_6)_2$ were prepared as described previously.[22,23] Solvents and ligands were used as received from the suppliers. All reactions were performed under an argon atmosphere. Column chromatography was carried out by using silica gel 60 (70−230 mesh) as the stationary phase and a 2% (v/v) solution of methanol in dichloromethane as the eluent unless otherwise stated. Purification of $[Ru(tpy)_2](PF_6)_2$ and analytical determination of purity for $[Ru(tpy)(4\text{-}Etpy)_3](PF_6)_2$ (**7**) was accomplished by using cation exchange HPLC with an Aquapore CX-300 column (1.0 × 10.0 cm) of poly(DL-Asp)-silica (Brownlee) with an elution gradient of 0−400 mM KBr in 2:3 (v/v) CH_3CN/0.6 mM phosphate buffer (pH = 7.2).

General Measurements. ^1H NMR spectra were recorded on a Bruker AC200 spectrometer, and all shifts are referenced to TMS. Elemental analyses were performed by ORS, Whitesboro, NY. UV−visible spectra were recorded by using either a Hewlett Packard Model 8451 A diode array spectrophotometer or an Olis modified Cary 14 spectrophotometer interfaced to an IBM microcomputer. Spectra were recorded on samples in 1.00 cm cells and were referenced against a solvent blank. All reported extinction coefficients are the average of values obtained at at least three different concentrations.

Synthesis of *trans*-$Ru(tpy)(PPh_3)(CF_3CO_2)_2$ (1). A solution of $AgCF_3CO_2$ (134 mg, 0.60 mmol) in acetone (25 mL) was added to a partial solution of *trans*-$Ru(tpy)(PPh_3)Cl_2$ (200 mg, 0.30 mmol) in dichloromethane (10 mL). The mixture was heated to 40 °C on an oil bath, and the dichloromethane was driven off over a period of 2 h, during which time AgCl precipitated. Further acetone (25 mL) was added and the solution filtered through Celite. The filtrate was evaporated to a volume of 5 mL and the product precipitated by the addition of diethyl ether. The solid was collected by filtration, washed with diethyl ether, and dried in air to yield **1** as a dark gray powder (123 mg, 50%): δ_H (CD_3COCD_3) 8.51−8.31 (6 H, m), 8.10 (1 H, t, J = 8.2 Hz), 7.88 (2 H, td, J = 7.8, 1.6 Hz), 7.80−7.70 (6 H, m), 7.51−7.33 (9 H, m), 7.11−7.05 (2 H, m). Anal. Calcd for $C_{37}H_{26}F_6N_3O_4Ru$: C, 54.02; H, 3.19; N, 5.11. Found: C, 53.59; H, 3.21; N, 5.00.

Synthesis of *trans*-$[Ru(tpy)(4\text{-}Etpy)_2(PPh_3)](PF_6)_2$ (2). 4-Ethylpyridine (0.1 mL) was added to a partial solution of **1** (100 mg, 0.122 mmol) in 1:1 (v/v) ethanol/water (40 mL). The mixture was heated to 65 °C on an oil bath and stirred for 5 h to yield an orange-brown solution. This was cooled to room temperature and filtered to remove a small amount of black solid, and aqueous NH_4PF_6 was added to the filtrate. Removal of the ethanol in vacuo afforded an orange-brown precipitate. Dichloromethane (10 mL) was added, and the dark orange organic layer separated. The aqueous layer was extracted several times with 10 mL portions of dichloromethane, and the combined organic extracts were evaporated to dryness. Purification of the crude product was achieved by column chromatography. The major orange band was collected, evaporated to dryness, and recrystallized from dichloromethane/diethyl ether to afford red-orange crystals of **2** (50 mg, 37%): δ_H (CD_2Cl_2) 8.46 (4 H, d, J = 8.2 Hz), 8.28−8.11 (5 H, m), 7.60−7.22 (21 H, m), 6.65 (4 H, d, J = 6.5 Hz), 2.47 (4 H, q, J = 7.6 Hz), 1.04 (6 H, t, J = 7.6 Hz). Anal. Calcd for $C_{47}H_{44}F_{12}N_5P_3Ru$: C, 51.28; H, 4.03; N, 6.36. Found: C, 50.96; H, 3.91; N, 6.33.

Synthesis of *trans*-$[Ru(tpy)(DMAP)_2(PPh_3)](PF_6)_2$ (3). This salt was prepared and purified in identical fashion to **2** by using **1** (80 mg, 0.097 mmol) and 4-(dimethylamino)pyridine (DMAP, 63 mg, 0.516 mmol) in place of 4-ethylpyridine. Acetone/dichloromethane (10% (v/v)) was used as the eluent for column chromatography. This afforded dark purple crystals of **3** (47 mg, 43%): δ_H (CD_2Cl_2) 8.39 (4 H, d, J = 8.1 Hz), 8.21−8.04 (5 H, m), 7.60−7.22 (17 H, m), 6.84 (4 H, d, J = 7.3 Hz), 6.06 (4 H, d, J = 7.3 Hz), 2.81 (12 H, s). Anal. Calcd for $C_{47}H_{46}F_{12}N_7P_3Ru$: C, 49.92; H, 4.10; N, 8.67. Found: C, 49.50; H, 4.06; N, 8.86.

Synthesis of $[Ru(tpy)(4\text{-}Etpy)(PPh_3)Cl]PF_6$ (4). To a suspension of $Ru(tpy)(PPh_3)Cl_2$ (253 mg, 0.38 mmol) in 1:1 (v/v) ethanol/water (100 mL) was added $TlPF_6$ (300 mg, 0.86 mmol). This mixture was heated under reflux for 2 h and then cooled to room temperature to yield a turbid orange-brown solution. 4-Ethylpyridine (0.1 mL) was added and the reaction mixture stirred at room temperature for 20 h. After this time the mixture was filtered and the ethanol evaporated from the filtrate, causing a dark precipitate to form. The crude product was isolated and purified as for **2** to afford **4** as dark red crystals (238 mg, 71%): δ_H (CD_2Cl_2) 9.14 (2 H, dd, J = 4.9 and 0.6 Hz), 7.97−7.66 (9 H, m), 7.46−7.39 (2 H, m), 7.30−7.07 (15 H, m), 6.84 (2 H, d, J = 5.7 Hz), 2.44 (2 H, q, J = 7.6 Hz), 1.03 (3 H, t, J = 7.6 Hz). Anal. Calcd for $C_{40}H_{35}ClF_6N_4P_2Ru$: C, 54.34; H, 3.99; N, 6.34. Found: C, 54.25; H, 3.94; N, 6.28.

Synthesis of *cis*-$[Ru(tpy)(4\text{-}Etpy)_2(PPh_3)](PF_6)_2$ (5). 4-Ethylpyridine (0.1 mL) was added to a partial solution of **4** (50 mg, 0.057 mmol) and $AgCF_3CO_2$ (15 mg, 0.068 mmol) in 1:1 (v/v) ethanol/water (100 mL). The mixture was heated at 75 °C on an oil bath for 2 h to yield a turbid orange solution. This was cooled to room temperature and filtered to remove the AgCl. Following the addition of aqueous NH_4PF_6, the crude product was isolated and purified as for **2** to afford orange crystals of **5** (57 mg, 92%): δ_H (CD_2Cl_2) 8.59 (2 H, d, J = 5.6 Hz), 8.27 (2 H, d, J = 6.5 Hz), 8.13−7.95 (8 H, m), 7.75−7.67 (2 H, m), 7.42−7.31 (4 H, m), 7.19−7.04 (8 H, m), 6.91 (2 H, d, J = 5.9 Hz), 6.53−6.43 (6 H, m), 2.86 (2 H, q, J = 7.6 Hz), 2.48 (2 H, q, J = 7.6 Hz), 1.35 (3 H, t, J = 7.6 Hz), 1.02 (3 H, t, J = 7.6 Hz). Anal. Calcd for $C_{47}H_{44}F_{12}N_5P_3Ru$: C, 51.28; H, 4.03; N, 6.36. Found: C, 50.91; H, 3.94; N, 6.30.

Synthesis of *trans*-$[Ru(tpy)(4\text{-}Etpy)_2Cl]PF_6$ (6). A suspension of $Ru(tpy)Cl_3$ (50 mg, 0.113 mmol) in 4-ethylpyridine (10 mL) was heated at 110 °C on an oil bath for 2 h. The red-brown solution was cooled to room temperature and evaporated to give an oily magenta residue. This was dissolved in methanol (2 mL), and the addition of aqueous NH_4PF_6 yielded a dark precipitate. The crude product was isolated and purified as for **2** to afford deep magenta crystals of **6** (65 mg, 79%): δ_H (CD_2Cl_2) 9.32 (2 H, d, J = 4.7 Hz), 8.33−8.26 (4 H, m), 8.05−7.69 (9 H, m), 6.77 (4 H, d, J = 6.7 Hz), 2.44 (4 H, q, J = 7.6 Hz), 1.03 (6 H, t, J = 7.6 Hz). Anal. Calcd for $C_{29}H_{29}ClF_6N_5PRu \cdot 0.25CH_2Cl_2$: C, 46.82; H, 3.96; N, 9.33. Found: C, 46.91; H, 3.91; N, 9.32.

Synthesis of $[Ru(tpy)(4\text{-}Etpy)_3](PF_6)_2$ (7). A partial solution of $Ru(tpy)Cl_3$ (100 mg, 0.227 mmol) and 4-ethylpyridine (2 mL) in 1:1 (v/v) ethanol/water (50 mL) was heated under reflux for 8 h. The red-brown solution was cooled to room temperature and evaporated to a volume of about 10 mL, and the product was precipitated by the addition of aqueous NH_4PF_6. The crude product was isolated and purified as for **2** to yield brown crystals of **7** (184 mg, 86%): δ_H (CD_2Cl_2) 8.63 (2

(19) (a) Amouyal, E.; Mouallem-Bahout, M.; Calzaferri, G. *J. Phys. Chem.* **1991**, *95*, 7641. (b) Amouyal, E.; Mouallem-Bahout, M. *J. Chem. Soc., Dalton Trans.* **1992**, 509.
(20) Constable, E. C.; Cargill-Thompson, A. M. W.; Armaroli, N.; Balzani, V.; Maestri, M. *Polyhedron* **1992**, *11*, 2707.
(21) (a) Allen, G. H.; Sullivan, B. P.; Meyer, T. J. *J. Chem. Soc., Chem. Commun* **1981**, 793. (b) Calvert, J. M.; Caspar, J. V.; Binstead, R. A.; Westmoreland, T. D.; Meyer, T. J. *J. Am. Chem. Soc.* **1982**, *104*, 6620.
(22) Sullivan, B. P.; Calvert, J. M.; Meyer, T. J. *Inorg. Chem.* **1980**, *19*, 1404.
(23) Constable, E. C. *J. Chem. Soc., Dalton Trans.* **1985**, 2687.

H, d, J = 5.0 Hz), 8.42 (4 H, d, J = 8.1 Hz), 8.19–8.05 (5 H, m), 7.86–7.78 (2 H, m), 7.56 (2 H, d, J = 6.5 Hz), 7.28 (4 H, d, J = 5.4 Hz), 6.88 (4 H, d, J = 6.6 Hz), 2.91 (2 H, q, J = 7.6 Hz), 2.50 (4 H, q, J = 7.6 Hz), 1.40 (3 H, t, J = 7.6 Hz), 1.06 (6 H, t, J = 7.6 Hz). Anal. Calcd for $C_{36}H_{38}F_{12}N_6P_2Ru{\cdot}0.25CH_2Cl_2$: C, 45.03; H, 4.01; N, 8.69. Found: C, 45.00; H, 3.96; N, 8.66.

Electrochemistry. Cyclic voltammetric measurements were carried out by using either a PAR Model 173 or a Par 273 potentiostat/galvanostat coupled to an in-house manufactured programmer. The measurements were carried out in a three compartment cell with the SCE reference electrode separated from the Pt disk working electrode (surface area 0.031 cm^2) and Pt wire auxiliary electrode by a medium-porosity glass frit. Spectrophotometric grade acetonitrile (Burdick and Jackson) was used as received and tetra-*n*-butylammonium hexafluorophosphate, [N(*n*-C_4H_9)$_4$]PF_6, doubly recrystallized from ethanol and dried in vacuo, was used as supporting electrolyte. Solutions containing 10^{-3} M analyte (0.1 M electrolyte) were deaerated for 15–20 min by a vigorous Ar purge. Sweep rates employed ranged from 20 to 1000 mV s^{-1}. All $E_{1/2}$ values were calculated from $(E_{pa} + E_{pc})/2$ at a scan rate of 200 mV s^{-1} with no correction for junction potentials.

Photophysical Measurements. Samples for lifetime and emission experiments were prepared as optically dilute solutions (OD < 0.5 at the λ_{max} in a 1.00 cm cell) in freshly distilled 4:1 (v/v) EtOH/MeOH, freeze–pump–thaw degassed for at least three cycles, and then sealed under vacuum. Visible spectra were recorded on all samples before and after measurements to check for photodecomposition.

Emission lifetimes at 77 K were obtained by using a liquid N_2 finger dewar or at variable temperatures by using a Janis Model NDT-6 cryostat coupled to a Lakeshore DRC-84C temperature controller. A PRA LN1000 pulsed nitrogen laser was used as an excitation source at 337 nm coupled to a PRA grating LN102/1000 tunable dye head laser. All lifetimes were obtained with 480 nm excitation by using Exciton Coumarin 480 as the laser dye. The excitation beam was passed through a collection of lenses and defocused onto the sample cell. Scattered light was removed by a dichromate cut-off filter. Emission decay was monitored at right angles with a PRA B204-3 2.5 monochromator and a Hammamatsu R928 water-cooled photomultiplier tube. Either a LeCroy 9400, 7200, or 9360 digitizing oscilloscope was used to collect the kinetic data. An IBM PC or Gateway 2000 microcomputer was employed for the kinetic analyses. Reported lifetimes are the average of 150–200 decay traces, were independent of monitoring wavelength, and could be satisfactorily fit to first-order decay.

Emission spectra were recorded on a Spex Fluorolog F212 photon-counting spectrofluorimeter equipped with either a R636, R928, or R666-98 red sensitive Hammamatsu phototube. All spectra were corrected for detector sensitivity. For all samples the emission spectral profiles were independent of excitation wavelength, and the excitation profiles were found to be independent of monitoring wavelength.

The determination of emission quantum yield relative to an external standard was calculated by using eq 1, in which A is the absorbance of

$$\phi_{em} = \left[\frac{A_r I_s}{A_s I_r}\right]\left[\frac{n_s}{n_r}\right]^2 \phi_r \qquad (1)$$

the sample at the excitation wavelength, I is the integrated intensity of the emission band, n is the refractive index of the solvent, ϕ_r is the emission quantum yield of the reference, and the subscripts r and s refer to the external reference and standard, respectively. Previously it has been observed, for 4:1 (v/v) EtOH/MeOH, that the increased absorbance at lower temperature due to solvent contraction is roughly compensated by an increase in the refractive index as the density increases, and ϕ_{em} varies directly as I as the temperature is changed.[24]

Emission Spectral Fitting. Emission spectra were normalized and the emission abscissa was converted to an abscissa linear in energy by the method of Parker and Rees.[25] Emission spectral fits were carried out by a modification of the previously described procedures and protocols[24,26] by using a simplex optimization routine.[27] All fits were performed on a Gateway 2000 microcomputer by using the two mode Franck–Condon analysis in eq 2.

$$I(\bar{\nu}) = \sum_{v_M=0}^{5}\sum_{v_L=-hb}^{15}\left\{\left(\frac{E_{00} - v_M\hbar\omega_M - v_L\hbar\omega_L}{E_{00}}\right)^3\left(\frac{S_M^{v_M}}{v_M!}\right)\times I(v_L)\exp\left[-4\ln 2\left(\frac{\bar{\nu} - E_{00} + v_M\hbar\omega_M + v_L\hbar\omega_L}{\Delta\bar{\nu}_{1/2}}\right)^2\right]\right\} \qquad (2)$$

$$E_0 = E_{00} - S_L\hbar\omega_L \qquad (3)$$

The Laguerre polynomials are defined by

$$I(n) = S_L^n\sum_{m=0}^{\infty}\left|\frac{X_m m!}{(m+n)!}\right|\left[\sum_{l=0}^{m}\frac{(m+n)!(-S_L)^l}{(m-l)!(l+n)!m!}\right]^2 \qquad (4)$$

$$I(-n) = X^n I(n) \qquad (5)$$

$$X = \exp\left(\frac{-\hbar\omega_L}{k_B T}\right) \qquad (6)$$

In eq 2 $I(\bar{\nu})$ is the emitted light intensity at energy $\bar{\nu}$ (in cm^{-1}) relative to I for the v_M^*, $v_L^* = 0 \rightarrow v_M$, $v_L = 0$ transition. v_M^*, v_L^* and v_M, v_L are vibrational quantum numbers for averaged medium- and low-frequency acceptor modes of quantum spacing $\hbar\omega_M$ and $\hbar\omega_L$ in the excited and ground states, respectively (the superscript denotes the excited state). The summations were carried out over 5 medium-frequency and 15 low-frequency vibrational levels and 5 hot bands whose contributions are included through $I(v_L)$. The quantities E_0 (eq 3) and E_{00} (eq 2) are the energy gaps (in cm^{-1}) between the excited and ground states for the ($v_M^* = 0$ to $v_M = 0$) and ($v_M^* = 0$, $v_L^* = 0$ to $v_M = 0$, $v_L = 0$) transitions, respectively. The quantities S_M and S_L are the Huang–Rhys factors (electron–vibrational coupling constants) for the medium- and low-frequency acceptor modes. The Huang–Rhys factor is related to the difference in the equilibrium displacements between the excited and ground states (ΔQ_e) and the reduced mass M by eq 7.

$$S = {}^1/_2\left(\frac{M\omega}{\hbar}\right)(\Delta Q_e)^2 \qquad (7)$$

The quantities S_M, $\hbar\omega_M$ and S_L, $\hbar\omega_L$ are averaged parameters for the contributions of a series of medium-frequency ring-stretching vibrations and a series of low-frequency vibrations, respectively. The term $\Delta\bar{\nu}_{1/2}$ is the full width at half-maximum (fwhm) for each of the vibronic components that appear in the emission spectra. In the fitting procedure $\hbar\omega_M$ and $\hbar\omega_L$ were fixed and E_{00}, S_M, S_L, and $\Delta\bar{\nu}_{1/2}$ were allowed to vary until the program found a minimum in the squared sum of the residuals.

Resonance Raman Spectra. Resonance Raman spectra were recorded at room temperature in CH_3CN with excitation at 457.9 nm. Sample concentration was *ca.* 10^{-4} M. The source was a Spectra-Physics Model 165 Ar^+ CW laser. The scattered light was dispersed by a Jobin Yvon U1000 double monochromator and detected by a Hammamatsu R943–02 cooled photomultiplier tube. Signal processing was accomplished with an Instruments SA Spectra Link photon-counting system. The spectra were an average of 16 accumulations with a spectral resolution of 4 cm^{-1}.

Results

Synthesis and Characterization. Reaction of Ru(tpy)Cl_3 with pyridine (py) in refluxing chloroform containing Et_3N as

(24) (a) Worl, L. A.; Duesing, R.; Chen, P.; Della Ciana, L.; Meyer, T. J. *J. Chem. Soc., Dalton Trans.* **1991**, 849. (b) Kober, E. M.; Caspar, J. V.; Lumpkin, R. S.; Meyer, T. J. *J. Phys. Chem.* **1986**, *90*, 3722.

(25) (a) Parker, C. A.; Rees, W. T. *Analyst (London)* **1960**, *85*, 857. (b) Allen, G. H.; White, R. P.; Rillema, D. P.; Meyer, T. J. *J. Am. Chem. Soc.* **1984**, *106*, 2613.

(26) (a) Caspar, J. V.; Meyer, T. J. *Inorg. Chem.* **1983**, *22*, 2444. (b) Caspar, J. V.; Westmoreland, T. D.; Allen, G. H.; Bradley, P. G.; Meyer, T. J.; Woodruff, W. H. *J. Am. Chem. Soc.* **1984**, *106*, 3492. (c) Barqawi, K. R.; Murtaza, Z.; Meyer, T. J. *J. Phys. Chem.* **1991**, *95*, 47.

(27) Claude, J.-P.; Meyer, T. J. Manuscript in preparation.

reductant gives *trans*-Ru(tpy)(py)Cl_2.[22] After extended periods of reflux in ethanol/water with pyridine, Ru(tpy)Cl_3 is converted into $[Ru(tpy)(py)_3]^{2+}$.[16] Reflux of *trans*-Ru(tpy)(PPh_3)Cl_2 in pyridine produces *trans*-$[Ru(tpy)(py)_2Cl]^+$, reaction of which with 4-methylpyridine (4-Mepy) in ethanol/water affords *trans*-$[Ru(tpy)(py)_2(4\text{-}Mepy)]^{2+}$.[16]

We find that, in refluxing 4-ethylpyridine (4-Etpy), *trans*-Ru(tpy)(PPh_3)Cl_2 is converted into *trans*-$[Ru(tpy)(4\text{-}Etpy)_2Cl]^+$, which was isolated as the PF_6^- salt **6** in high yield. Ru(tpy)Cl_3 reacts similarly under these conditions, also affording **6** in comparable yield. The salt, $[Ru(tpy)(4\text{-}Etpy)_3](PF_6)_2$ (**7**), was prepared from Ru(tpy)Cl_3 by a procedure similar to that previously reported for $[Ru(tpy)(py)_3](PF_6)_2$.[16]

Silver(I) trifluoroacetate ($AgCF_3CO_2$) was used to remove both chlorides of *trans*-Ru(tpy)(PPh_3)Cl_2 under relatively mild conditions to afford *trans*-Ru(tpy)(PPh_3)$(CF_3CO_2)_2$ (**1**) in reasonable yield. **1** was used to synthesize the symmetrical *trans*-bis-(py-R) derivatives *trans*-$[Ru(tpy)(py\text{-}R)_2(PPh_3)](PF_6)_2$ (py-R = 4-Etpy (**2**) or py = DMAP (**3**)) by gentle heating in ethanol/water containing an excess of the appropriate pyridyl ligand. These reactions were not highly efficient, but fair yields of **2** and **3** were isolated following column chromatography. Reaction of **1** under similar conditions with a variety of other substituted pyridyl ligands including 4,4′-bipyridine and 4-nitropyridine failed to afford any identifiable products. The reaction between **1** and 4-Etpy was attempted at room temperature in a variety of solvents including dichloromethane, ethanol/water, methanol, acetone, acetonitrile, and DMF. In all cases either no reaction was observed or an intractable product mixture was produced after a period of 7 days. Hence compound **1** has a somewhat limited potential as a precursor to complexes of the type *trans*-$[Ru(tpy)(py)_2(PPh_3)]^{2+}$.

Reaction of *trans*-Ru(tpy)(PPh_3)Cl_2 with 1 equiv of $AgCF_3CO_2$ in refluxing ethanol/water containing 4-Etpy gave a mixture of three isomers of $[Ru(tpy)(4\text{-}Etpy)(PPh_3)Cl]^+$ (*vide infra*) together with the disubstituted *trans* complex **2**. The product distribution was found to shift in favor of the latter by using excess $AgCF_3CO_2$ and/or larger concentrations of 4-Etpy, but complex mixtures were invariably obtained.

Reaction of excess thallium(I) hexafluorophosphate ($TlPF_6$) with *trans*-Ru(tpy)(PPh_3)Cl_2 in refluxing ethanol/water appeared to yield a mono-aqua intermediate.[28] Its subsequent reaction with 4-Etpy at room temperature gave a high yield of a monosubstituted complex isolated as a salt of formulation $[Ru(tpy)(4\text{-}Etpy)(PPh_3)Cl]PF_6$ (**4**). Only trace amounts of other products were observed during chromatography. In the absence of structural data the coordination geometry of **4** is uncertain (*vide infra*), but ^1H NMR showed that only a single isomer of the three possible was present. Further reaction of **4** with $AgCF_3CO_2$ in the presence of 4-Etpy afforded exclusively a disubstituted complex isolated as the salt *cis*-$[Ru(tpy)(4\text{-}Etpy)_2(PPh_3)](PF_6)_2$ (**5**).

The reaction between *trans*-Ru(tpy)(PPh_3)Cl_2 and $TlPF_6$ was also carried out in refluxing ethanol/water in the presence of an excess of 4-Etpy. This afforded a product mixture which was partially resolved by column chromatography on silica gel with 2% (v/v) methanol/dichloromethane as the eluent. The major purple product fraction was analyzed by TLC on silica gel and separated into three components with 5% (v/v) acetone/dichloromethane. The first was the red product **4** isolated from the reaction in which the chloride was removed in the absence of 4-Etpy. The second component was a mauve color, and the third, which was a deep purple-brown, constituted the major part of the fraction taken from the column.

^1H NMR spectroscopy in dichloromethane confirmed that the chromatographed sample contained a mixture of the three isomeric complexes having the formula $[Ru(tpy)(4\text{-}Etpy)(PPh_3)Cl]^+$. This was most clearly seen in the ethyl region of the spectrum. The signals at 2.44 and 1.03 ppm, a quartet and triplet respectively, were due to the red isomer **4** isolated previously. Another set of signals, a quartet at 2.85 ppm and a triplet at 1.35 ppm, were assigned to the second mauve component observed by TLC. A third set of multiplets, a quartet at 2.29 ppm and a triplet at 0.97 ppm, were assigned to the third and predominant, purple-brown isomer shown by TLC. The combined yield of monosubstituted complexes was in excess of 50%, but an appreciable quantity of the disubstituted complex **2** was also produced in this reaction.

The syntheses of the new complexes **1**−**7** are shown in Scheme 1.

Absorption Spectra. Absorption spectra and band assignments are given in Table 1, and the spectrum of $[Ru(tpy)(4\text{-}Etpy)_3](PF_6)_2$ (**7**) is shown in Figure 1. Assignments were made by comparison to $[Ru(tpy)_2]^{2+}$ and related Ru(II) mono-(tpy) complexes,[16,29] and the well-documented MLCT transitions found for $[Ru(bpy)_3]^{2+}$.[6] The visible bands are $d\pi \rightarrow \pi^*$, MLCT in character. They are broad because they include a series of MLCT transitions and their vibronic components. The UV bands arise from $\pi \rightarrow \pi^*$ intraligand transitions with the $\pi \rightarrow \pi^*$ tpy bands in $[Ru(tpy)_2]^{2+}$ appearing at 308, 272, 225, and 198 nm. Additional, overlapping UV absorptions appear from $\pi \rightarrow \pi^*$ transitions in the 4-Etpy and PPh_3 ligands.

Electrochemistry. $E_{1/2}$ values for $Ru^{III/II}$ and $tpy^{0/-}$ redox couples are listed in Table 1. The $Ru^{III/II}$ waves are chemically reversible as evidenced by peak current ratios (i_{pa}/i_{pc}) of unity, scan rate independent peak to peak separations (ΔE_p) of 70−80 mV, and linear correlations between peak currents and the square root of the scan rate for $\nu = 50-1000$ mV s^{-1}. The first tpy-based reductions in *trans*-$[Ru(tpy)(4\text{-}Etpy)_2Cl]PF_6$ (**6**) and $[Ru(tpy)(4\text{-}Etpy)_3](PF_6)_2$ (**7**) at −1.42 and −1.24 V were, at best, quasi-reversible as evidenced by an increase in ΔE_p as the scan rate was increased. A second, irreversible reduction wave near the solvent limit (-1.9 to −2.0 V in CH_3CN) was observed for all complexes but not investigated in detail.

For the complexes containing PPh_3 a more complex reductive behavior was observed as illustrated for *trans*-$[Ru(tpy)(4\text{-}Etpy)_2(PPh_3)](PF_6)_2$ (**2**) in Figure 2. Irreversible reductions appear at $E_{p,c} = -1.11$, −1.26, and −1.53 V as well as an anodic wave at −0.3 V on the return scan. Potential switching studies show that the oxidative wave at −0.3 V is observed only after scanning through the second reductive wave at −1.26 V. If the potential is switched at −1.22 V, a return wave for the first reduction at −1.11 V becomes prominent at scan rates greater than 200 mV s^{-1}. In addition, the current response for the second reduction decreases with increasing scan rate. These observations are consistent with a one electron reduction followed by a coupled chemical reaction, presumably ligand substitution.

Emission and Emission Spectral Fitting. Room-temperature measurements in CH_3CN or 4:1 (v/v) EtOH/MeOH for $[Ru(tpy)(4\text{-}Etpy)_3](PF_6)_2$ (**7**) and *cis*- and *trans*-$[Ru(tpy)(4\text{-}Etpy)_2(PPh_3)](PF_6)_2$ (**5** and **2**) show that these complexes are short-lived, weak emitters. They are photochemically unstable toward ligand loss as shown by changes in UV−visible spectra upon

(28) It is possible that the removal of Cl^- could generate a five-coordinate intermediate, $[Ru(tpy)(PPh_3)Cl]^+$, but reaction of this would be expected to yield a mixture of isomers rather than the observed clean formation of **4** in greater than 70% yield.

(29) Leising, R. A.; Kubow, S. A.; Churchill, M. R.; Buttrey, L. A.; Ziller, J. W.; Takeuchi, K. J. *Inorg. Chem.* **1990**, *29*, 1306.

Scheme 1. Synthesis of Mono(terpyridine)ruthenium(II) Complexes

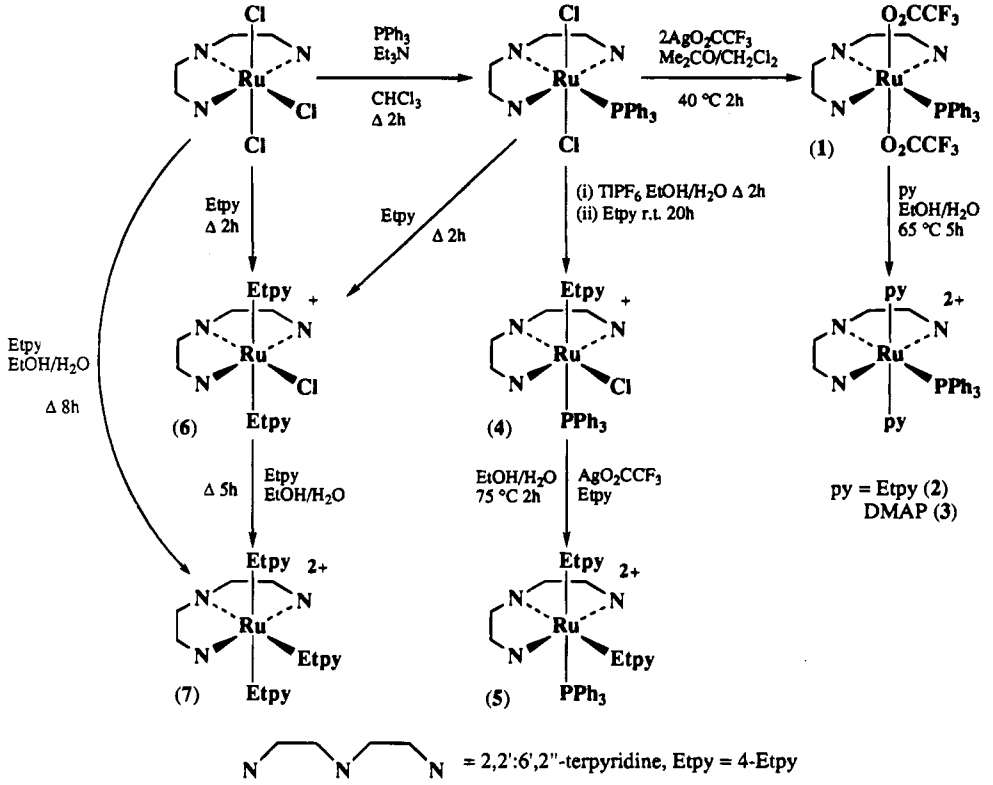

photolysis. Ligand loss from $[Ru(tpy)(py)_3]^{2+}$ in acetone containing Cl^- occurs with $\phi_p = 0.037$.[16] Higher quantum yields for ligand loss are found for *cis*-$[Ru(bpy)_2(py)_2]^{2+}$ ($\phi_p = 0.20$)[30] and $[Ru(bpy)_3]^{2+}$ ($\phi_p = 0.062$)[31] but with measurements made in CH_2Cl_2.

Emission spectra at 77 K and spectra calculated by use of the spectral fitting parameters in Table 2 by application of eq 2 are shown in Figure 3. Also presented in Table 2 are emission lifetimes, maxima, and, where available, emission quantum yields along with literature data for $[Ru(bpy)_3]^{2+}$ for comparative purposes.

Temperature Dependent Quantum Yields and Emission Lifetimes. The temperature dependences of the relative emission quantum yields and lifetimes for $[Ru(tpy)_2](PF_6)_2$ and $[Ru(tpy)(4\text{-Etpy})_3](PF_6)_2$ (**7**) are shown in Figure 4.[32] In the limit of a single emitting state (or a multiplet of states acting as a single state) with a nonemitting state above it contributing to nonradiative decay, emission quantum yields and lifetimes are given by

$$\phi_{em} = k_r\tau = k_r[k_0 + k_1 \exp(-\Delta E_1/k_BT)]^{-1} \quad (8)$$

$$\tau^{-1} = k_{obs} = k_0 + k_1 \exp(-\Delta E_1/k_BT) \quad (9)$$

In eqs 8 and 9 $k_0 = k_r + k_{nr}$, where k_r and k_{nr} are the rate constants for radiative and nonradiative decay, respectively, from the emitting MLCT states. It is assumed that the temperature dependence of k_0 is negligible, that the emitting states are reached with unit efficiency, and that the upper state is not appreciably populated.[33] The quantities k_1 and ΔE_1 are kinetic parameters characterizing transition and decay through the higher state. The lifetime data for **7** were fit to eq 9, and the kinetic parameters are listed in Table 3 along with literature values for $[Ru(tpy)_2]^{2+}$, $[Ru(bpy)_3]^{2+}$, and *cis*-$[Ru(bpy)_2(py)_2]^{2+}$ for comparative purposes.

The fits of the temperature dependent data were extended to just above the glass to fluid transition (120−140 K). As observed previously, decay kinetics are complex in the glass to fluid region. This occurs because of a kinetic coupling between excited state decay and relaxation of the surrounding solvent dipoles.[34] At 116 K, decay traces were slightly nonexponential but independent of monitoring wavelength. At 130 K emission decay was biexponential and wavelength dependent with the emission maximum shifting to the red as relaxation of the solvent dipoles occurred.

Resonance Raman Spectra. The resonance Raman (RR) spectrum of $[Ru(tpy)_2]^{2+}$ acquired at 298 K in CH_3CN by using 457.9 nm excitation is shown in Figure 5. Data for $[Ru(tpy)_2]^{2+}$ along with literature data for $[Ru(bpy)_3]^{2+}$ and $[Os(bpy)_3]^{2+}$ are summarized in Table 4. Previous studies on $[Os(bpy)_3]^{2+}$ and $[Ru(bpy)_3]^{2+}$ have shown that the bpy modes that experience the greatest enhancements are a series of symmetrical ν(bpy) vibrations from 1000 to 1600 cm^{-1}.[26b,35] A series of resonantly enhanced bands are found in the same region for $[Ru(tpy)_2]^{2+}$, although the pattern is more complex.

(30) Pinnick, D. V.; Durham, B. *Inorg. Chem.* **1984**, *23*, 1440.
(31) Durham, B.; Caspar, J. V.; Nagle, J. K.; Meyer, T. J. *J. Am. Chem. Soc.* **1982**, *104*, 4803.
(32) The data shown in Figure 4 are the normalized relative emission intensities for $[Ru(tpy)_2](PF_6)_2$ and **7** in 4:1 (v/v) EtOH/MeOH. They are plotted as $I(T)/I(90)$ for $[Ru(tpy)_2](PF_6)_2$ and $I(T)/I(115)$ for **7** where $I(T)$, $I(90)$, and $I(115)$ are the integrated emission intensities at temperatures T, 90, and 115 K, respectively. The data are internally consistent for each complex and illustrate the temperature dependence of the emission intensity; however, the absolute magnitudes of the integrated emission intensities for $[Ru(tpy)_2](PF_6)_2$ and **7** are not comparable.
(33) Lumpkin, R. S.; Kober, E. M.; Worl, L. A.; Murtaza, Z.; Meyer, T. J. *J. Phys. Chem.* **1990**, *94*, 239.
(34) (a) Kitamura, N.; Kim, H.-B.; Kawanishi, Y.; Obata, R.; Tazuke, S. J. *J. Phys. Chem.* **1986**, *90*, 1488. (b) Danielson, E.; Lumpkin, R. S.; Meyer, T. J. *J. Phys. Chem.* **1987**, *91*, 1305.
(35) (a) McClanahan, S. F.; Kincaid, J. R. *J. Raman Spectrosc.* **1984**, *15*, 173. (b) Danzer, G. D.; Kincaid, J. R. *J. Phys. Chem.* **1990**, *94*, 3976 and references therein.

Table 1. UV−Visible and Electrochemical Data in CH_3CN

complex[a]	E, V vs SCE[b] $E_{1/2}$- ($Ru^{III/II}$)	$E_{1/2}$- ($tpy^{0/-}$)	λ_{max},[c] nm (ϵ, M^{-1} cm^{-1})	assign
$[Ru(tpy)_2]^{2+}$	1.30[d]	−1.24[d]	476 (14 800)	$d\pi \rightarrow \pi^*$
			438 (8800)	$d\pi \rightarrow \pi^*$
			325 (28 400) sh	$d\pi \rightarrow \pi^*$
			308 (64 300)	$\pi \rightarrow \pi^*$
			272 (38 600)	$\pi \rightarrow \pi^*$
			225 (36 100) sh	$\pi \rightarrow \pi^*$
$[Ru(tpy)(4\text{-}Etpy)_3]^{2+}$ (**7**)	1.24	−1.25	610 (560) sh	$d\pi \rightarrow \pi^*$
			550 (1930) sh	$d\pi \rightarrow \pi^*$
			504 (5400)	$d\pi \rightarrow \pi^*$
			450 (4500) sh	$d\pi \rightarrow \pi^*$
			318 (35 800)	$\pi \rightarrow \pi^*$
			274 (21 500)	$\pi \rightarrow \pi^*$
			238 (26 700)	$\pi \rightarrow \pi^*$
			210 (32 700)	$\pi \rightarrow \pi^*$
trans-$[Ru(tpy)(4\text{-}Etpy)_2Cl]^+$ (**6**)	0.76	−1.42	593 (2990) sh	$d\pi \rightarrow \pi^*$
			548 (5500)	$d\pi \rightarrow \pi^*$
			493 (4130) sh	$d\pi \rightarrow \pi^*$
			358 (13 000) sh	$d\pi \rightarrow \pi^*$
			318 (34 600)	$\pi \rightarrow \pi^*$
			276 (21 800)	$\pi \rightarrow \pi^*$
			238 (24 900)	$\pi \rightarrow \pi^*$
trans-$[Ru(tpy)(DMAP)_2(PPh_3)]^{2+}$ (**3**)	1.07	−1.13	486 (3950)	$d\pi \rightarrow \pi^*$
			320 (44 700)	$\pi \rightarrow \pi^*$
			284 (34 700)	$\pi \rightarrow \pi^*$
			276 (35 600)	$\pi \rightarrow \pi^*$
			209 (74 500)	$\pi \rightarrow \pi^*$
trans-$[Ru(tpy)(4\text{-}Etpy)_2(PPh_3)]^{2+}$ (**2**)	1.44	−1.18[e]	550 (860) sh	$d\pi \rightarrow \pi^*$
			474 (3000) sh	$d\pi \rightarrow \pi^*$
			448 (3500)	$d\pi \rightarrow \pi^*$
			338 (14 400) sh	$d\pi \rightarrow \pi^*$
			320 (22 400)	$\pi \rightarrow \pi^*$
			288 (16 900)	$\pi \rightarrow \pi^*$
			278 (16 000)	$\pi \rightarrow \pi^*$
			206 (75 200)	$\pi \rightarrow \pi^*$
cis-$[Ru(tpy)(4\text{-}Etpy)_2(PPh_3)]^{2+}$ (**5**)	1.42	−1.23[e]	460 (4050)	$d\pi \rightarrow \pi^*$
			425 (3200) sh	$d\pi \rightarrow \pi^*$
			335 (13 400) sh	$d\pi \rightarrow \pi^*$
			312 (26 100)	$\pi \rightarrow \pi^*$
			282 (18 700)	$\pi \rightarrow \pi^*$
			232 (33 900)	$\pi \rightarrow \pi^*$
$[Ru(tpy)(4\text{-}Etpy)(PPh_3)Cl]^+$ (**4**)	0.89	−1.43	476(4050)	$d\pi \rightarrow \pi^*$
			314 (27 300)	$\pi \rightarrow \pi^*$
			276 (16 400)	$\pi \rightarrow \pi^*$
			232 (27 000)	$\pi \rightarrow \pi^*$

[a] As PF_6^- salts. [b] In CH_3CN 0.1 M in $[N(n\text{-}C_4H_9)_4]PF_6$. [c] In CH_3CN at room temperature (>200 nm). [d] From ref 18. [e] Reduction is followed by ligand dissociation; see text for details.

Discussion

Synthesis and Characterization. The experiments involving direct substitution of chloride by 4-ethylpyridine (4-Etpy) have demonstrated that it is not necessary to form *trans*-Ru(tpy)-$(PPh_3)Cl_2$ to prepare symmetrical *trans*-$[Ru(tpy)(py)_2Cl]^+$ complexes under relatively forcing reaction conditions. However, this reaction is useful only if a pyridyl ligand is used as the solvent, and hence this approach is severely limited for preparing *trans* pyridyl complexes.

The bis(trifluoroacetate) precursor **1** has also provided a route to *trans* complexes but again in only limited fashion. In these reactions both *trans* axial ligands are substituted, although no attempt was made to isolate monosubstituted intermediates. Symmetrical complexes such as **2** have also been produced in variable quantities from reactions in which assisted chloride loss occurs in the presence of a pyridyl ligand. These reactions feature a very low degree of substitutional control, isomers are produced, and careful column chromatography is necessary to separate often complex product mixtures. The abstraction of a single chloride to form an isomerically pure monosubstituted complex, a prerequisite for the preparation of asymmetrical complexes, was achieved by using thallium(I). Hence the monochloro complex salt **4** has been isolated and efficiently converted into the *cis*-disubstituted complex salt **5** by abstraction of the second chloride by silver(I). This represents the only case in which a sequential substitution of chlorides has been achieved but with a loss of the desired *trans* stereochemistry.

The presence of two sets of ethyl resonances of equal intensity in the ^1H NMR spectrum of **5** is proof of the *cis* geometry, and this has been confirmed by a single crystal X-ray structure determination.[36] The isolation of the *cis* complex indicates that migration of PPh_3 takes place either during the initial substitution step to form **4** or during the second step to form **5**. It is most likely that this occurs during the first substitution which occurs at a higher temperature than the second step.

In an attempt to avoid this undesirable rearrangement, the abstraction of a single chloride from *trans*-$Ru(tpy)(PPh_3)Cl_2$ by thallium(I) was carried out in the presence of 4-Etpy. However, instead of affording a single substitution product in which the PPh_3 remained in the equatorial position, this reaction gave a mixture of the three possible isomers of $[Ru(tpy)(4\text{-}Etpy)(PPh_3)Cl]^+$, as evidenced by both TLC and ^1H NMR. By comparison with the positions of the ethyl resonances in the other 4-Etpy complexes, it is possible to suggest structures for the three isomers (Figure 6). The first, red isomer (isomer 1), which was isolated and characterized fully as the salt **4**, has a quartet and triplet at shifts which are very close to the ethyl resonances for axial 4-Etpy *trans* to 4-Etpy in the salts *trans*-$[Ru(tpy)(4\text{-}Etpy)_2X](PF_6)_n$ (**2**, X = PPh_3, n = 2, δ 2.47 and 1.04 ppm; **6**, X = Cl^-, n = 1, δ 2.44 and 1.03 ppm; **7**, X = 4-Etpy, n = 2, δ 2.50 and 1.06 ppm). Variation of X in the series **2**, **6**, **7** has only a slight influence on the 4-Etpy resonances. This suggests that the 4-Etpy in isomer 1 is also axial, but it may be *trans* to PPh_3 or Cl^-. The similarity in ethyl shifts for isomer 1 to the signals at 2.48 and 1.02 ppm for axial 4-Etpy *trans* to PPh_3 in *cis*-$[Ru(tpy)(4\text{-}Etpy)_2(PPh_3)](PF_6)_2$ (**5**) suggests that isomer 1 contains 4-Etpy *trans* to PPh_3 and therefore Cl^- in the equatorial site.

The second, mauve isomer (isomer 2) has resonances which are close to those for equatorial 4-Etpy in $[Ru(tpy)(4\text{-}Etpy)_3](PF_6)_2$ (**7**) at 2.91 and 1.40 ppm and coincident with those in **5** at 2.86 and 1.35 ppm. These resonances are relatively insensitive to the nature of the axial ligands. Hence isomer 2 is likely to contain 4-Etpy in the equatorial position.

The ethyl resonances for the third and predominant, purple-brown isomer (isomer 3) appear at 2.29 and 0.97 ppm, to high field of all of those observed in the other isomers. If the earlier assignments are correct, this isomer must contain axial 4-Etpy *trans* to Cl^-. The high degree of shielding is consistent with *trans* Cl^- acting as a pπ-donor.

Isomer 1 is, therefore, derived from reaction of $[Ru(tpy)(PPh_3)(H_2O)Cl]^+$ in which the Cl^- is equatorial. This could result from an initial migration of PPh_3 followed by migration of Cl^- to fill the equatorial site (Scheme 2). Such a rearrangement is highly likely given the well-documented ease of dissociation and the steric bulk of the PPh_3 ligand.[37] The presence of an equatorial PPh_3 in the plane of the tpy may produce unfavorable steric interactions with the 6,6″ hydrogens of the tpy. Furthermore, the abstraction was carried out under relatively forcing conditions in the absence of 4-Etpy. Ad-

(36) Red crystals of **5** were grown by slow diffusion of diethyl ether vapor into a solution in dichloromethane. Crystal data: molecular formula $C_{47}H_{44}F_{12}N_5P_3Ru$; space group orthorhombic $P2_12_12_1$; unit cell parameters a = 13.405(3) Å, b = 14.318(4) Å, c = 25.249(11) Å. White, P. S. Unpublished results.

(37) Tolman, C. A. *Chem. Rev.* **1977**, *77*, 313.

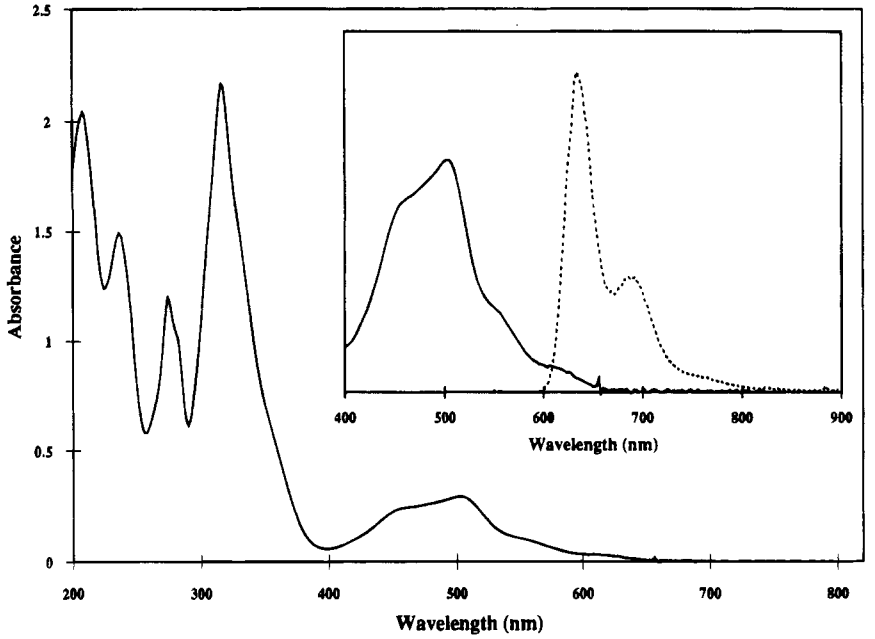

Figure 1. UV−visible spectrum of $[Ru(tpy)(4\text{-}Etpy)_3](PF_6)_2$ (**7**) in CH_3CN solution at room temperature. Inset: Absorption in CH_3CN (—) and emission intensity in arbitrary units (- - -) at 77 K in 4:1 (v/v) EtOH/MeOH.

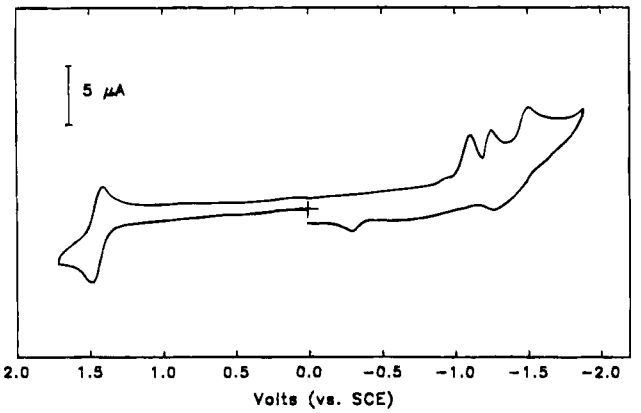

Figure 2. Cyclic voltammogram of *trans*-$[Ru(tpy)(4\text{-}Etpy)_2(PPh_3)](PF_6)_2$ (**2**) in CH_3CN ($[N(n\text{-}C_4H_9)_4PF_6]$ = 0.1 M) at a scan rate of 200 mV s^{-1}.

ditional evidence for the structural assignment for isomer 1 is found in the electrochemical data for **4** (*vide infra*).

By inference, isomer 3 is the desired precursor for the preparation of asymmetrical *trans* complexes in which initial substitution has occurred with retention of the *trans* stereochemistry. In order to utilize isomer 3 as a precursor to further *trans* complexes, it is first necessary to obtain it in a pure form since contamination by the other isomers causes formation of *cis* products by further substitution, and these are not readily separated from the desired *trans* complexes. Rigorous attempts at purification by column chromatography, recrystallization, and even HPLC failed to give a pure sample of the desired isomer, as shown by ^1H NMR. Some separation of isomers could be observed chromatographically, but it appears that isomer 3 readily converts to the other two. Whether this occurs thermally or photochemically is unclear.

Electrochemistry. Although the $Ru^{III/II}$ potentials show very little dependence on coordination geometry as evidenced by the similar values for the *cis* and *trans* isomers **5** and **2**, the first tpy-based reduction is particularly sensitive to the nature of the equatorial ligand. This is shown by the data in Table 1 where the shift in $E_{1/2}$ changing from Cl^- (in **6**) to 4-Etpy (in **7**) in the equatorial position is +170 mV and the shift from equatorial Cl^- to PPh_3 (in **2**) is +240 mV. Comparison of $E_{1/2}$ values for the *cis* and *trans* isomers in **5** and **2** shows that replacing equatorial 4-Etpy by PPh_3 causes a shift of +50 mV. The highly cathodic tpy reduction at −1.43 V for **4** is the same as for **6**, and this is consistent with the suggestion that **4** contains equatorial Cl^-, in agreement with the conclusions reached by ^1H NMR (*vide supra*).

Electronic Structure. The MLCT States. The photophysical data acquired are revealing as to structure and dynamics in tpy-based MLCT excited states. Emission energies are sensitive to the nonchromophoric ligands, shifting to higher energy as $\Delta E_{1/2}$ ($E_{1/2}(Ru^{III/II}) - E_{1/2}(Ru^{II}(tpy)/Ru^{II}(tpy^{\bullet-})$) increases. Plots of $\Delta E_{1/2}$ (at 298 K in CH_3CN) vs E_{em} (at 77 K in 4:1 (v/v) EtOH/MeOH) are linear (slope = 4860 cm^{-1} V^{-1}, R = 0.975) which is an expected and characteristic feature for MLCT excited states.[38] The existence of the linear correlation is good evidence that the emitting excited state is MLCT in character throughout the series.

$E_{1/2}$ values for the first ligand-based reductions in CH_3CN are −1.33 V for $[Ru(bpy)_3]^{2+}$ [39] and −1.24 V for $[Ru(tpy)_2]^{2+}$.[18] This suggests that it is easier to reduce tpy than bpy by *ca.* 0.1 V.

Absorption spectra include well-defined, low-energy shoulders that overlap with emission (Figure 1). These bands arise from $^1[(d\pi)^6] \rightarrow {}^3[(d\pi)^5(\pi^*)^1]$ transitions which are allowed due to spin−orbit coupling which has the effect of mixing excited singlet and triplet states.[40] Analysis of the spectrum of $[Ru(tpy)(4\text{-}Etpy)_3](PF_6)_2$ (**7**) (Figure 1) shows that the energy difference between the lowest, intense singlet, $^1[(d\pi)^6] \rightarrow {}^1[(d\pi)^5(\pi^*)^1]$, band at 504 nm (19 840 cm^{-1}) and the triplet $^1[(d\pi)^6] \rightarrow {}^3[(d\pi)^5(\pi^*)^1]$ band at ~610 nm (~16 400 cm^{-1}) is 3400 cm^{-1}, which is of similar magnitude to the singlet−triplet splitting energy for $[Ru(bpy)_3]^{2+}$.[40] Similar energy differences exist for the other mono-tpy complexes. Although the low-

(38) (a) Barqawi, K. R.; Llobet, A.; Meyer, T. J. *J. Am. Chem. Soc.* **1988**, *110*, 7751. (b) Kober, E. M.; Marshall, J. L.; Dressick, W. J.; Sullivan, B. P.; Caspar, J. V.; Meyer, T. J. *Inorg. Chem.* **1985**, *24*, 2755.
(39) Bock, C. R.; Connor, J. A.; Gutierrez, A. R.; Meyer, T. J.; Whitten, D. G.; Sullivan, B. P.; Nagle, J. K. *J. Am. Chem. Soc.* **1979**, *101*, 4815.
(40) Kober, E. M.; Meyer, T. J. *Inorg. Chem.* **1982**, *21*, 3967.

Table 2. Emission and Lifetime Data in 4:1 (v/v) EtOH/MeOH at 77 K and Spectral Fitting Parameters from Eq 2[a]

complex[b]	λ_{max},[em] nm (ϕ_{em})[c]	τ, μs	E_0, E_{00}, cm^{-1}	$\hbar\omega_M$, $\hbar\omega_L$, cm^{-1}	S_M, S_L	$\Delta\bar{\nu}_{1/2}$, cm^{-1}
$[Ru(bpy)_3]^{2+}$	584, 630 (0.38)	5.2	16 940, 17 380(10)	1400, 400	1.0(0.009), 1.1(0.04)	575(20)
$[Ru(tpy)_2]^{2+}$	599, 648 (0.48)	11.0	16 400, 16 820(8)	1250, 350	0.7(0.008), 1.2(0.03)	423(18)
$[Ru(tpy)(4\text{-}Etpy)_3]^{2+}$ (**7**)	634, 689	7.5	15 620, 15 840(5)	1250, 350	0.5(0.003), 0.6(0.02)	634(8)
cis-$[Ru(tpy)(4\text{-}Etpy)_2(PPh_3)]^{2+}$ (**5**)	624, 650 sh	5.8	16 070, 16 940(19)	1150, 350	0.7(0.007), 2.5(0.07)	547(32)
trans-$[Ru(tpy)(4\text{-}Etpy)_2(PPh_3)]^{2+}$ (**2**)	606, 658	4.9	16 220, 16 580(11)	1320, 360	0.8(0.008), 1.0(0.05)	587(23)
trans-$[Ru(tpy)(DMAP)_2(PPh_3)]^{2+}$ (**3**)	683, 714	1.1				

[a] With standard deviations for variable parameters in parentheses. [b] As PF_6^- salts. [c] λ_{max} for the first two vibronic features.

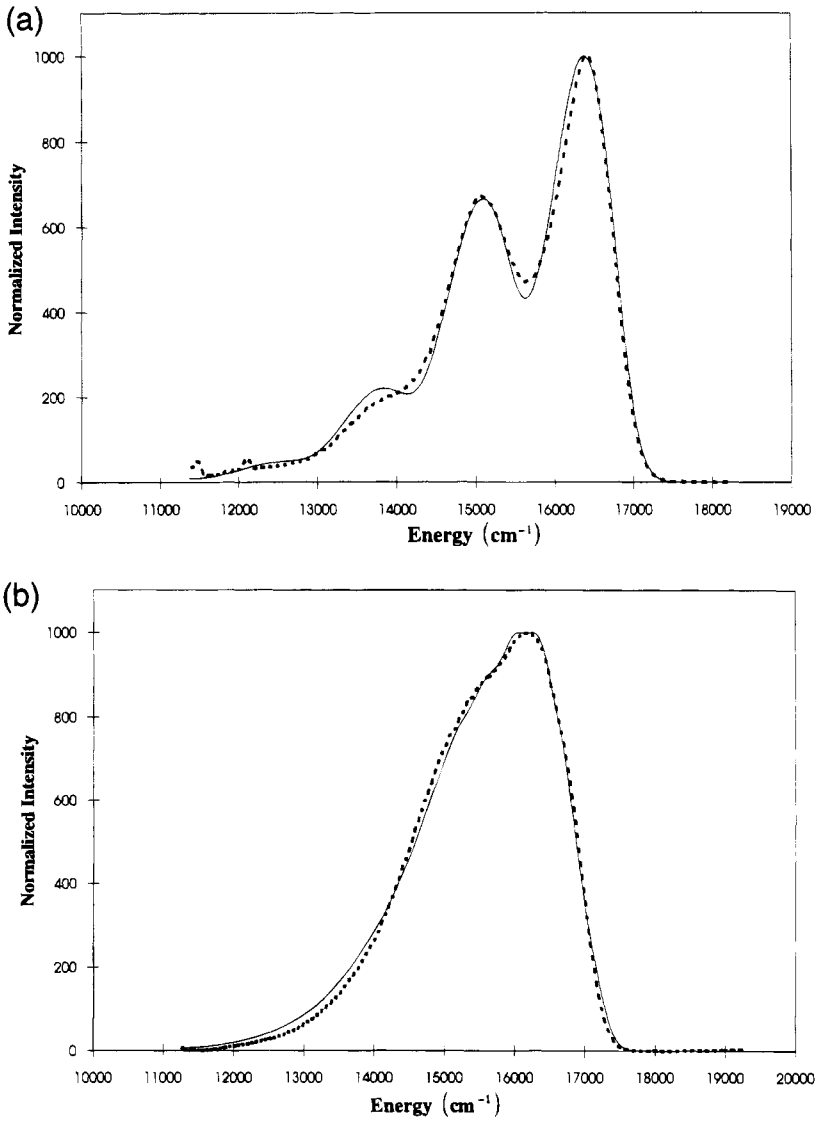

Figure 3. Emission spectrum (—) and calculated best fit (- - -) by using eq 2 and the spectral fitting parameters in Table 2 at 77 K in 4:1 (v/v) EtOH/MeOH for (a) *trans*-$[Ru(tpy)(4\text{-}Etpy)_2(PPh_3)](PF_6)_2$ (**2**) and (b) *cis*-$[Ru(tpy)(4\text{-}Etpy)_2(PPh_3)](PF_6)_2$ (**5**).

energy bands are badly overlapped with the low-energy part of the singlet manifold, their absorptivities appear to be enhanced; $\epsilon \sim 400$ M^{-1} cm^{-1} for $[Ru(tpy)_2]^{2+}$ at 600 nm compared to $\epsilon \sim 100$ M^{-1} cm^{-1} for $[Ru(bpy)_3]^{2+}$. This may be due to enhanced mixing with low-lying $\pi\pi^*$ states given the more complex electronic structure of the tpy ligand.

2,2′,2″-Terpyridine as the Acceptor Ligand. The pattern of participating vibrations for tpy as the acceptor ligand is revealed in the resonance Raman spectrum in Figure 5. In addition to the usual bpy-based enhancements for $[M(bpy)_3]^{2+}$ (M = Ru(II) or Os(II)) (Table 4), resonantly enhanced Raman bands for $[Ru(tpy)_2]^{2+}$ are observed at 1549, 1470, 1164 (or 1183), and 728 cm^{-1}. The relative intensity of the band at 673 cm^{-1} is significantly enhanced compared to its analogs in the tris-bpy series.

In 77 K emission spectral fits of $[Ru(tpy)_2]^{2+*}$ and $[Ru(tpy)\text{-}(4\text{-}Etpy)_3]^{2+*}$ satisfactory fits were obtained with $\hbar\omega_M = 1250$ cm^{-1} and $\hbar\omega_L = 350$ cm^{-1} (Table 2). In these fits S_M and $\hbar\omega_M$ are averaged quantities for the contributions by a series of ring skeletal modes above 1000 cm^{-1}. The common value for $\hbar\omega_M$ points to a common pattern of acceptor vibrations for these complexes. The magnitude of $\hbar\omega_M$ is 50−150 cm^{-1} lower than commonly found for related bpy complexes[24,26] because of the contribution of the additional vibrations below 1183 cm^{-1}.

There is evidence for greater delocalization of the excited electron in tpy compared to bpy from the decreased magnitude

(41) (a) Boyde, S.; Strouse, G. F.; Jones, W. E., Jr.; Meyer, T. J. *J. Am. Chem. Soc.* **1990**, *112*, 7395. (b) Strouse, G. F.; Schoonover, J. R.; Duesing, R.; Boyde, S.; Jones, W. E., Jr.; Meyer, T. J. *Inorg. Chem.*, in press.

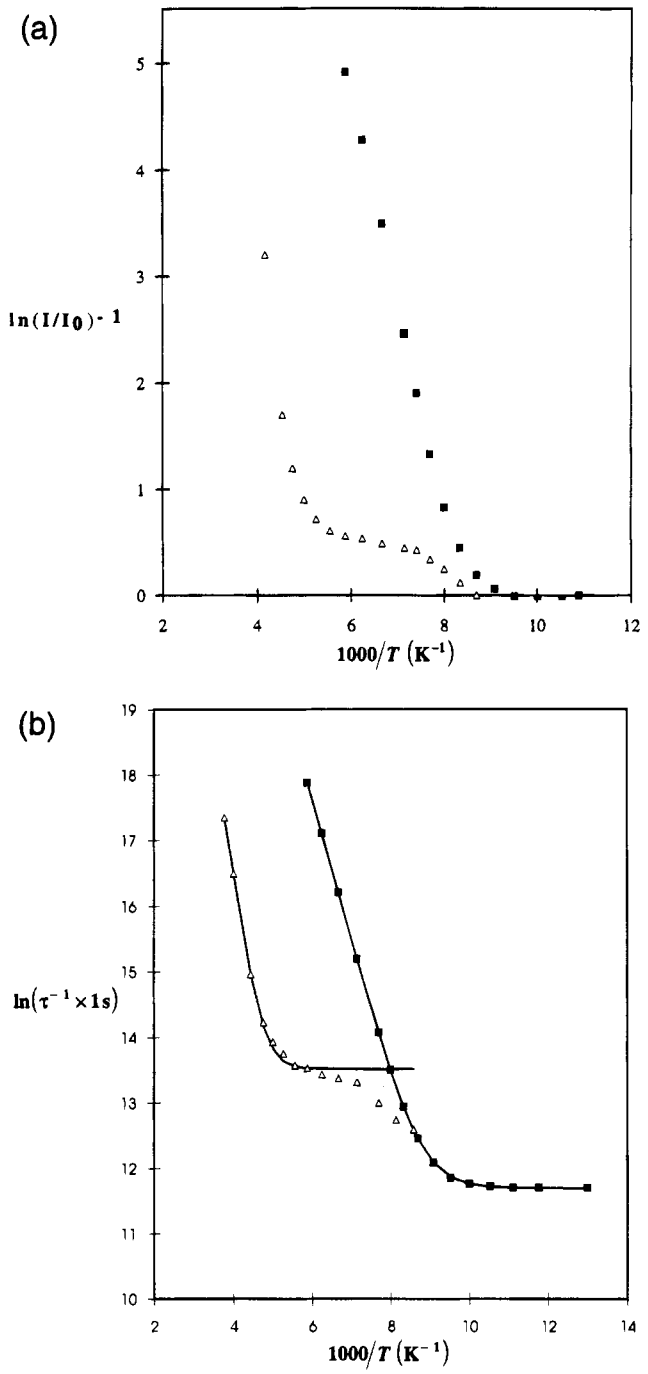

Figure 4. (a) Temperature dependent relative quantum yields[32] for $[Ru(tpy)(4\text{-}Etpy)_3](PF_6)_2$ (**7**, △) and $[Ru(tpy)_2](PF_6)_2$ (■) in 4:1 (v/v) EtOH/MeOH. (b) Temperature dependent emission lifetimes for **7** (△) and $[Ru(tpy)_2](PF_6)_2$ (■) in 4:1 (v/v) EtOH/MeOH. The latter were calculated from the kinetic parameters in ref 17 by using eq 9.

of S_M for tpy. This is expected since the electron is delocalized over three pyridyl rings rather than two. The effects of enhanced delocalization on structural changes and nonradiative lifetimes in MLCT excited states have been discussed previously.[41] S_M is related to the change in equilibrium bond displacements between the ground and excited states in the averaged ν(bpy) acceptor vibration, ΔQ_e, by eq 7. Delocalization over a larger molecular framework causes a decrease in ΔQ_e. This can be seen for tpy as the acceptor by comparing $[Ru(bpy)_3]^{2+}$ and *cis*-$[Ru(tpy)(4\text{-}Etpy)_2(PPh_3)]^{2+}$ (Table 2) which are closest to having the same energy gap, where S_M decreases from 1.0 to 0.7. Assuming the same reduced mass, this leads to a ΔQ_e ratio of $(1.0/0.7)^{1/2} = 1.20$ from eq 7 and a decrease in the local bond displacements that contribute to the averaged normal mode.

Table 3. Photochemical and Photophysical Parameters

complex[a]	ϕ_p[b]	ϕ_{em}	τ, ns	$10^{-5}k_0$, s^{-1}[c]	$10^{-13}k_1$, s^{-1}[c]	ΔE_1, cm^{-1}[c]
$[Ru(bpy)_3]^{2+}$	0.062[d]	0.029[e]	490[e]	3.9[f]	19[f]	3860[f]
cis-$[Ru(bpy)_2(py)_2]^{2+}$	0.20[g]	n.e.[f]	2.7[f]	4.2[f]	23[f]	2760[f]
$[Ru(tpy)_2]^{2+}$	n.o.	n.e.[h]	0.25[h]	1.2[i]	1.9[i]	1500[i]
$[Ru(tpy)(4\text{-}Etpy)_3]^{2+}$	0.037[j]	weak	4.0[k]	7.4	8.5	2720

[a] As PF_6^- salts, except for $[Ru(bpy)_3]^{2+}$ as Cl^- salt for ϕ_p measurement only. n.e. = nonemissive. n.o. = none observed; see text for details. [b] Quantum yields for ligand loss with Cl^- as incoming ligand. [c] From the temperature dependence of τ according to eq 9 in 4:1 (v/v) EtOH/MeOH. [d] From ref 31; measured in CH_2Cl_2. [e] From ref 26a; measured in deoxygenated CH_2Cl_2. [f] From ref 46. [g] From ref 30; measured in CH_2Cl_2 and independent of $[Cl^-]$ from 5×10^{-4}–10^{-2} M. [h] From ref 14; measured in H_2O. [i] From ref 17. [j] From ref 16; for py loss from $[Ru(tpy)(py)_3]^{2+}$ measured in acetone. [k] Calculated by using eq 9.

The increase in $\hbar\omega_M$ for *trans*-$[Ru(tpy)(4\text{-}Etpy)_2(PPh_3)](PF_6)_2$ (**2**, $\hbar\omega_M = 1320\ cm^{-1}$) compared to its *cis* isomer **5** ($\hbar\omega_M = 1150\ cm^{-1}$) is also significant. The increase for the *trans* isomer is due to the electronic effect of having the π-acceptor ligand PPh_3 in the plane of tpy. A related effect was observed in the electrochemical data. Cross-axis π-bonding by $d\pi(p)$–$d\pi(Ru)$–$\pi^*(tpy)$ mixing may alter the character of the π^* level, lowering it in energy and causing more "localization" on the central pyridyl ring.

The vibrational characteristics of tpy as the acceptor ligand also influence nonradiative decay. In the limit of the applicability of the energy gap law the rate constant for nonradiative decay is given by[24b,42]

$$k_{nr} = \beta_0[F(\text{calcd})] \tag{10}$$

$$\ln(k_{nr} \times 1\text{s}) = \ln(\beta_0 \times 1\text{s}) + \ln[F(\text{calcd})] \tag{11}$$

In these equations β_0 is the vibrationally induced electronic coupling matrix element and F(calcd) the vibrational overlap term, for which[24]

$$F(\text{calcd}) \sim \exp[-(S)]\exp\left[-\left(\frac{\gamma E_0}{\hbar\omega_M}\right)\right] \tag{12}$$

where

$$\gamma = \ln\left(\frac{E_0}{S_M\hbar\omega_M}\right) - 1 \tag{13}$$

On the basis of this analysis, at least qualitatively, the decreases in S (and $\hbar\omega$) for tpy compared to bpy are expected to result in a decrease in F(calcd). Because of the decrease in excited state–ground state structural change, tpy is less effective as an acceptor ligand. Given the lifetimes in Table 2, if this is so the magnitude of β_0 must be increased for tpy compared to bpy. Microscopically, mixing of the states is induced by the promoting modes which have the appropriate symmetry to mix the electronic states. It is known from X-ray crystallographic studies that the tpy ligand does not span the full 180° of a terdentate, planar ligand. The angle formed between the two distal pyridyl nitrogens and the Ru center is typically between 155 and 160°.[29,43] An enhanced magnitude for β_0 may result from the lowered electronic symmetry with participation by additional low-frequency vibrations as promoting modes.

Temperature Dependence. Lifetimes of $[Ru(tpy)_2]^{2+*}$ and $[Ru(tpy)(4\text{-}Etpy)_3]^{2+*}$ decrease considerably with temperature

(42) (a) Englman, R.; Jortner, J. *Mol. Phys.* **1970**, *18*, 145. (b) Freed, K. F.; Jortner, J. *J. Chem. Phys.* **1970**, *52*, 6272.

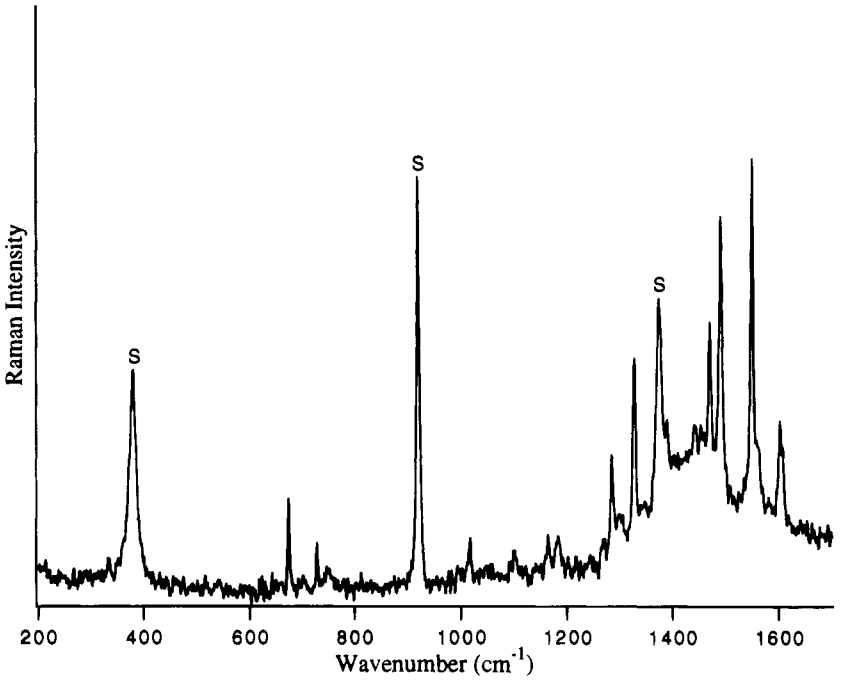

Figure 5. Resonance Raman spectrum of $[Ru(tpy)_2](PF_6)_2$ in CH_3CN solution at room temperature acquired by using 457.9 nm excitation. The spectrum is an average of 16 scans and has a spectral resolution of 4 cm^{-1}. The bands denoted S (at 379, 918, and 1374 cm^{-1}) are due to the solvent.

Table 4. Resonance Raman Band Energies (cm^{-1}) for $[M(bpy)_3]^{2+}$ (M = Ru(II) or Os(II))[a] and $[Ru(tpy)_2]^{2+}$ [b] Obtained with MLCT Excitation at Room Temperature

$[Ru(bpy)_3](PF_6)_2$ (λ_{ex} = 457.9 nm)	$[Os(bpy)_3](PF_6)_2$ (λ_{ex} = 488.0 nm)	$[Ru(tpy)_2](PF_6)_2$ (λ_{ex} = 457.9 nm)
1608	1608	1602
1563	1555	1559 sh
		1549
1493	1489	1490
		1470
1320	1321	1328
1276	1272	1284
	1259	
1175	1174	1183
		1164
1109	1110	1101
	1066	1094
	1047	
1030	1027	1018
768		748
		728
670	672	673

[a] From ref 35a; measured in 0.5 M aqueous Na_2SO_4. [b] Measured in CH_3CN.

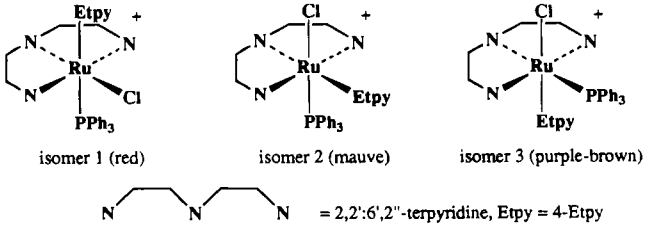

Figure 6. Proposed structures of the three isomers of $[Ru(tpy)(4\text{-}Etpy)(PPh_3)Cl]^+$ as identified by TLC and ^1H NMR spectroscopy.

as room temperature is approached. Their temperature dependences can be fit to eq 9. In other polypyridyl complexes of Ru(II) this effect has been attributed to a combination of thermal activation and decay from low-lying, metal-centered dd states and/or MLCT states having greater singlet character.[6b,6c,38] The parameters k_1 and ΔE_1 obtained from the fits are typical ($k_1 \sim 10^{13}-10^{14}$ s^{-1}; $\Delta E_1 \sim 2500-4000$ cm^{-1}) of cases where the temperature dependence is dominated by a MLCT → dd transition. In cases where decay via an upper MLCT state dominates, typical parameters are $k_1 \sim 10^7-10^8$ s^{-1} and $\Delta E_1 \sim 500-800$ cm^{-1}.[44]

The importance of thermal activation and decay through a dd state or states for $[Ru(tpy)(4\text{-}Etpy)_3]^{2+*}$ is reinforced by the appearance of ligand loss photochemistry, which has been studied quantitatively in $[Ru(tpy)(py)_3]^{2+}$, Table 3. ΔE_1 for $[Ru(tpy)_2]^{2+}$ (~1500 cm^{-1})[17] is significantly smaller, and yet there is no evidence for photosubstitution. Photolysis of $[Ru(tpy)_2]^{2+}$ in the presence of 0.1 M HCl results in no discernible photodecomposition under conditions where photolysis of $[Ru(bpy)_3]^{2+}$ gives $Ru(bpy)_2Cl_2$.[45] Presumably, MLCT → dd surface crossing occurs for $[Ru(tpy)_2]^{2+}$ as well, but the resulting dd state is not active toward ligand loss, at least at room temperature. This may be a result of a short dd excited state lifetime and/or a relatively high thermal barrier to ligand loss in the dd state.

In comparing $[Ru(bpy)_3]^{2+}$ with *cis*-$[Ru(bpy)_2(py)_2]^{2+}$, previous investigators[30,46] have shown that replacing bpy by py results in a decrease in ΔE_1. The energy gap ΔE_1 is smaller for

(43) (a) Deacon, D. B.; Patrick, J. M.; Skelton, B. W.; Thomas, N. C.; White, A. H. *Aust. J. Chem.* **1984**, *37*, 929. (b) Adcock, P. A.; Keene, F. R.; Smythe, R. S.; Snow, M. R. *Inorg. Chem.* **1984**, *23*, 2336. (c) Thummel, R. P.; Jahng, Y. *Inorg. Chem.* **1986**, *25*, 2527. (d) Seok, W. K. Ph.D. Thesis, University of North Carolina at Chapel Hill, 1988. (e) Lawson, H. J.; Janik, T. S.; Churchill, M. R.; Takeuchi, K. J. *Inorg. Chim. Acta* **1990**, *174*, 197. (f) Hecker, C. R.; Fanwick, P. E.; McMillin, D. R. *Inorg. Chem.* **1991**, *30*, 659. (g) Pramanik, A.; Bag, N.; Chakravorty, A. *J. Chem. Soc., Dalton Trans.* **1992**, 97. (h) Steed, J. W.; Tocher, D. A. *Inorg. Chim. Acta* **1992**, *191*, 29. (i) Constable, E. C.; Cargill Thompson, A. M. W.; Tocher, D. A.; Daniels, M. A. M. *New J. Chem.* **1992**, *16*, 855. (j) Grover, N.; Gupta, N.; Singh, P.; Thorp, H. H. *Inorg. Chem.* **1992**, *31*, 2014. (k) Chen, X. Ph.D. Thesis, University of North Carolina at Chapel Hill, 1992.

(44) Lumpkin, R. S.; Kober, E. M.; Worl, L. A.; Murtaza, Z.; Meyer, T. J. *J. Phys. Chem.* **1990**, *94*, 239.

(45) As detected by absorption spectral changes after photolysis in 50% (v/v) EtOH/0.1 M HCl with a Hg/Xe arc lamp for 3 h.

(46) Wacholtz, W. M.; Auerbach, R. A.; Schmehl, R. H.; Ollino, M.; Cherry, W. R. *Inorg. Chem.* **1985**, *24*, 1758.

Scheme 2. Suggested Reaction Sequence for Formation of Isomer 1

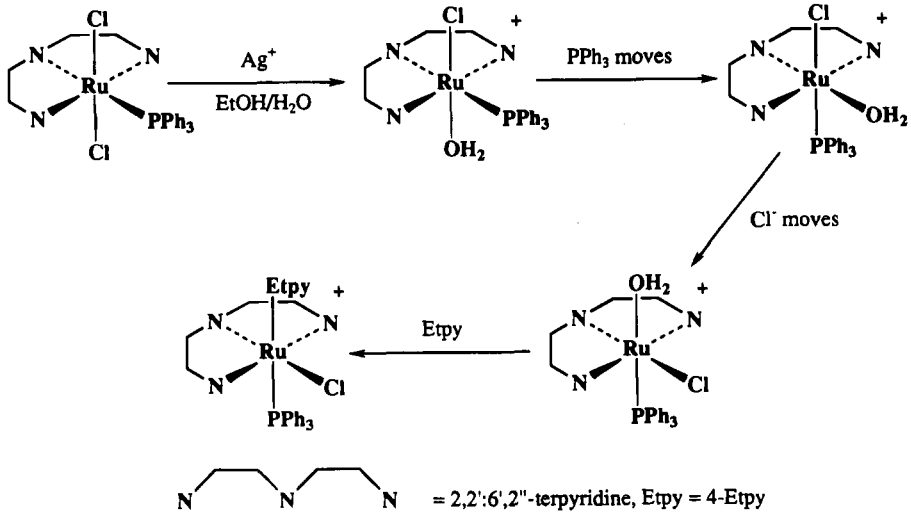

$[Ru(tpy)_2]^{2+}$ than for $[Ru(tpy)(4\text{-}Etpy)_3]^{2+}$. This may be a consequence of replacing the coordinatively restricted tpy ligand by three mondentate pyridyls. The lowered symmetry in $[Ru(tpy)_2]^{2+}$ caused by the N−Ru−N bite angle of 155−160° mixes $d\sigma^*$ and $d\pi$ orbitals, decreasing the energy of the lowest dd state.[21] When one of the tpy ligands is removed and replaced with three pyridyls, the geometrical restriction is partly lifted which may increase the MLCT-dd energy gap. This may be significant in the design of tpy-based MLCT excited states in which photosubstitution plays a lesser role.

On the basis of MO calculations on a series of bis(4′-phenylterpyridine)ruthenium(II) complexes,[19a] Amouyal *et al.* have argued that tpy-based excited state decay does not occur via a MLCT-dd state transition because the calculated energies of the $d\sigma^*$ antibonding orbitals are significantly higher in energy than the π^* levels of the substituted tpy ligand.[19] It was proposed instead that excited state decay at room temperature was due to participation in nonradiative decay by low-frequency intramolecular vibrations. The temperature dependence was explained as a consequence of these molecular motions being "frozen" out as the temperature was decreased. On the basis of our resonance Raman and emission spectral fitting results, this conclusion is incorrect. Nonradiative decay of the MLCT states, as described by eqs 10 and 11, is expected to be nearly temperature independent. The important acceptor modes are of relatively high frequency and populations above $v^* = 0$ are negligible even at room temperature. These are nearly activationless quantum transitions which cannot be "frozen out".

Summary

The preparation of symmetrical *trans*-$[Ru(tpy)(py)_2(PPh_3)]^{2+}$ complexes has been achieved, but in limited fashion, by using the bis(trifluoroacetate) precursor **1**. It appears that sequential substitution of the chloride ligands cannot be achieved without some degree of isomerization, resulting in loss of the desired *trans* stereochemistry. This is attributed in part to the tendency of the PPh_3 ligand to migrate to an axial site. Similar experiments with *trans*-$Ru(tpy)(PEt_3)Cl_2$ have indicated that this behavior may be a general problem with *trans*-$Ru(tpy)(PR_3)Cl_2$ complexes as potential precursors.[47]

On the basis of the photophysical studies, tpy complexes of Ru(II) appear to be more-or-less normal members of the larger family of polypyridyl chromophores, but with some special nuances of their own. Singlet → triplet MLCT transitions are clearly observed at low energy and with higher absorptivity than in bpy complexes. Greater delocalization of the excited electron causes a decrease in excited state distortion and a decrease in k_{nr}. The extent of delocalization depends on the ligand in the equatorial position relative to tpy, with the electron-withdrawing ligand PPh_3 causing enhanced localization on the central pyridyl. The small bite angle of tpy causes $d\sigma^*-d\pi^*$ mixing and a greater role for dd states in excited state decay. By a judicious choice of ligands, it may be possible to decrease photochemical ligand loss and provide a basis for the preparation of stable molecular assemblies for the study of photoinduced electron and energy transfer.

Acknowledgment. Support by the U.K. Science and Engineering Research Council under the NATO Postdoctoral Fellowship scheme (B.J.C.), the Natural Science and Engineering Research Council of Canada (D.W.T.), and the Department of Energy (Contract No. DE-FG05-86ER13633) is gratefully acknowledged. Thanks are due to Kimberly A. Opperman and Dr. Carlo A. Bignozzi for preliminary synthetic results, to Juan-Pablo Claude for the spectral fitting program, and to Juan-Pablo Claude and Estelle L. Lebeau for assistance with preparing figures. D.W.T. is grateful to Dr. Thomas R. Boussie for assistance with HPLC purifications and Darla K. Graff for many helpful discussions.

IC940289J

(47) Opperman, K. A.; Bignozzi, C. A.; Meyer, T. J. Unpublished results.